MAPPING KEY HYDROLOGICAL VARIABLES USING REMOTELY SENSED IMAGES INTEGRATED IN A DISTRIBUTED WATER BALANCE MODEL

N. Sánchez [a, *], J. Martínez-Fernández [a], A. Calera [b], E. Torres [b], C. Pérez-Gutiérrez [a]

[a] CIALE, Centro Hispano Luso de Investigaciones Agrarias. Universidad de Salamanca. Río Duero, 12; 37185 Villamayor (Salamanca), Spain - (nilda, jmf, carpegu)@usal.es
[b] IDR, Instituto de Desarrollo Regional. Universidad de Castilla La Mancha. Campus Universitario s/n, 02071 Albacete. Spain - (Alfonso.Calera, Enrique.Torres)@uclm.es

KEY WORDS: Modelling, Imagery, Landsat, Calibration, Classification

ABSTRACT:

A cartographic application of remotely sensed images integrated in a distributed water balance is presented. The imagery consisted in an annual series of Landsat 7 ETM+, from where the NDVI (Normalized Difference Vegetation Index) and the land uses/land cover (lu/lc) map were extracted. The soil database came from a permanent experimental network of 23 stations for continuous measurement of soil moisture (REMEDHUS, Soil Moisture Measurement Stations Network) at the Duero Basin (Spain). The theoretical basis of the water balance application derives from FAO56, which is improved with a spatial frame implemented in the computerized tool HIDROMORE. In addition to the image inputs, climatic and soil properties databases were also integrated. Maps of Actual Evapotranspiration (AET), Deep Percolation (DP), and Irrigation rates (I) were extracted. Soil moisture series were simulated for each REMEDHUS station, and the validation of the simulation was performed comparing simulated soil moisture against field-measured. The results for the area-average soil moisture are: RMSE (Root Mean Square Error)=0.02 cm^3cm^{-3}, AI (Agreement Index)=0.90 and R (correlation coefficient)=0.82. It was found that the parameters which showed the most influence in the maps appearance were the soil characteristics (water content at field capacity and at wilting point), precisely the parameters that most spatially vary and are the most difficult to acquire.

1. INTRODUCTION

Combining remotely sensed data with a water balance is a frequent approach in hydrological modeling. Images can be used to estimate the spatial distribution of the evapotranspiration of locations within the scene as well as regional distributions of water balance components (Wegehenkel and Kersebaum, 2005). Regarding FAO56 (Allen et al., 1998), the use of remotely sensed NDVI can improve the tabulated values of some calculation parameters (i.e., Fraction of Vegetation Cover (FVC), basal crop coefficient (K_{cb})), and the lu/lc map can assign spatial patterns to some others, such as irrigation rates, root depth, and plant height. The innovation of HIDROMORE is that it makes possible the integration of standard calculations of FAO56 with the spatial database resulting from Landsat (for vegetation parameters), plus the soil map (for soil parameters) and the map interpolated with the available weather stations (for climatic parameters). The operational aim of this application −conceived for calculating irrigation optimum rates close to real time− rules out highly complex methods of image treatment. Regarding the geometric correction, an RMSE smaller than pixel size is suitable for a correct recording of all the images (Wolfe et al., 2002; Schroeder et al., 2006). As for the radiometric correction, due to the complexity of knowing the atmospheric parameters, the use of Dark Object Sustraction (DOS) method is frequent (Chavez, 1989). The main objective of this research was to present a cartographic application of multitemporal remotely sensed images integrated in a distributed water balance model to derive maps of key hydrological variables that are useful for water management. Simple but effective processing methods of calibration, correction and classification of the multitemporal remotely sensed images were applied in order to integrate the results in the balance calculation. A second goal was to discuss the resulting maps and validate them with in-situ soil moisture

* Corresponding author

2. STUDY AREA, SOIL AND CLIMATE DATABASES

The study area is located in the central region of the Duero Basin, in the Castilla y León region of Spain (Figure 1). The climate is continental-Mediterranean, with around 400 mm of average annual precipitation. Mean temperature is 12 ºC, with long, cold winters and hot summers. The average annual potential evapotranspiration is 1025 mm according to Penman-Monteith method. Land uses are mainly crops.

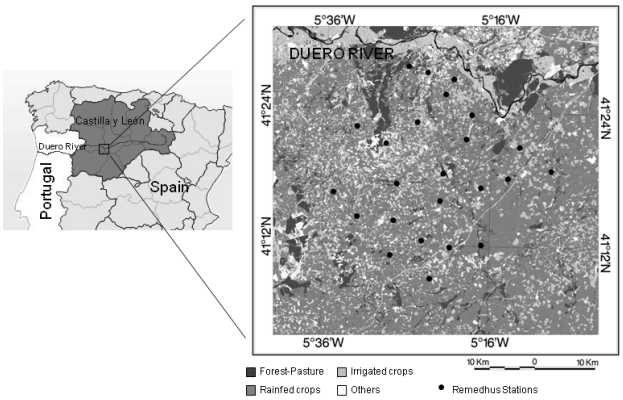

Figure 1. Lu/lc map of REMEDHUS area.

Distributed over 1300 km^2 the REMEDHUS network is made up of 23 stations for the measurement and monitoring of soil moisture (Martínez-Fernández and Ceballos, 2005). The soil database has a grid distribution of 3x3 km^2. For each one of these cells (146), several parameters are known at surface level: texture and water content at field capacity (θ_{FC}), at wilting point (θ_{WP}) and at saturation (θ_{sat}). The climatic database (precipitation, P, and Penmann-Monteith-based reference

evapo-transpiration, ET_0) came from one automatic weather station located in the REMEDHUS network.

3. MATERIAL AND METHODS

3.1 Image processing

A series of Landsat 7 ETM+ images from 2002 was used, scene 202/031, L1G path-oriented level. The series covered the whole year and allowed the study of the growing season of rainfed crops (spring) and irrigated crops (summer-autumn). All the scenes were clear and free of clouds.

For the geometric corrections, the physical model (Toutin, 2004) was chosen, based on the Landsat 7 orbital parameters and 24 ground control points, as well a digital elevation model of 1 m resolution, and the nearest neighbour resampling method. The global bundle adjustment showed an RMSE(X) of 0.68 pixels and RMSE(Y) of 0.70 pixels for all the images altogether.

The radiometric calibration and atmospheric correction were performed for red and infrared bands on each date. The procedure consisted of one-step transformation, following the method proposed by Pons and Solé-Sugrañés (1994). This method computes standard values of solar irradiance, calculated distance sun-earth, and standard values of aerosol optical depth for the red and infrared bands. DOS methods and topographic correction were also integrated.

Due to the difficulty of having a useful map during the study period, the spatial patterns of occupation of land are usually derived from remotely sensed maps. In this study, Landsat-derived map of lu/lc is used for: a) assigning the root depth, b) identifying irrigated crops, and c) thresholding the plant height and K_{cb} for each class. Irrigated crops map is used for estimating the irrigation water required to avoid water stress in their area along the growing season. Two factors were taken into account when selecting the thematic categories of the lu/lc map: similar temporal evolution of the plant cover (based on the evolution of NDVI curves) and representativeness of classes for the study area. For this last choice, Corine Land Cover map of 2000 and statistics of the Geographic Information System for Agricultural Plots (SIGPAC) were consulted (75% rainfed grasslands, 9% irrigated grasslands, 11% forest-pasture, 2% vineyards). The six categories chosen were rainfed cereal crops, irrigated crops, unproductive, water, vineyards, and forest-pasture (pasture cover with scattered trees).

The strategy of classification depends on modeling requirements. As NDVI is the most effective single spectral dimension to derive land cover types (Cihlar et al., 1996), its temporal series were made the basis of the lu/lc classification, and each NDVI date was an input band. Regarding the algorithm, two methods were tested: segmentation of NDVI values (Vincent and Pierre, 2003) and the maximum likelihood algorithm applied to a supervised classification. The training areas were extracted mixing the SIGPAC database and a field campaign.

For validating the two maps, control plot error and confusion matrix were applied. The map resulting of the supervised procedure had a mean accuracy of 86,83% and the map resulting of the segmentation, one of 69,2%. The confusion matrix showed a mean accuracy of 79,81% and kappa (Lillesand and Kiefer, 1999) of 0,69 for the supervised map and 78,85% and kappa 0,63 for the segmented map. In summary, the best procedure seemed the supervised classification, so the lu/lc map resulting of it was chosen for the integration in HIDROMORE.

3.2 Modelling

3.2.1 Theoretical background: FAO56 procedure, also called K_cET_0 approach, calculates reference and crop evapotranspiration from meteorological data and crop coefficients (Allen, 1998). Using the dual crop coefficient approach, the calculation of AET is performed as:

$$AET=ET_0(K_sK_{cb}+K_e) \quad (1)$$

In this dual form, the term $K_sK_{cb}ET_0$, represents the transpiration component, and the term K_eET_0, represents the soil evaporation component. Basal crop coefficient, K_{cb}, is the transpiration coefficient at a potential rate, i.e. when water is not limiting transpiration, and it is usually obtained from tabulated values; K_s describes the effect of water stress, and it is calculated according the water content in the root layer, that it is estimated from a daily water balance. The soil evaporation coefficient, K_e, is calculated from the water balance on the upper soil surface layer.

The soil moisture content in the root layer was calculated as a residual value of the water balance equation, and can be expressed as a water deficit or depletion (D_r). The balance was daily calculated in the following way, for day i:

$$D_{r,i}=D_{r,i-1}-P_i-I_i+AET_i+DP_i \quad (2)$$

where $D_{r,i}$ is the depletion for day i; $D_{r,i-1}$ is the depletion for the day i-1; DP_i is deep percolation for the day i, or the amount of water that exceeds the field capacity; and P_i, I_i and AET_i are effective precipitation, irrigation rate and AET for the day i respectively. Surface runoff was not considered in the current application.

The above described approach, which was developed initially for crops under optimal management conditions, can be also applied to natural or non-pristine vegetation (Allen et al., 1998). The problem in this case is how to obtain K_{cb} for crops or vegetation out of perfect growing conditions. The solution applied in this paper for solving this, is to obtain the time series of K_{cb} from the time series of NDVI, applying a previously developed relationship NDVI-K_{cb}. To obtain NDVI daily values, we interpolate linearly from the dates where the image is available. The schema of the application and other intermediate parameters are shown in Figure 2.

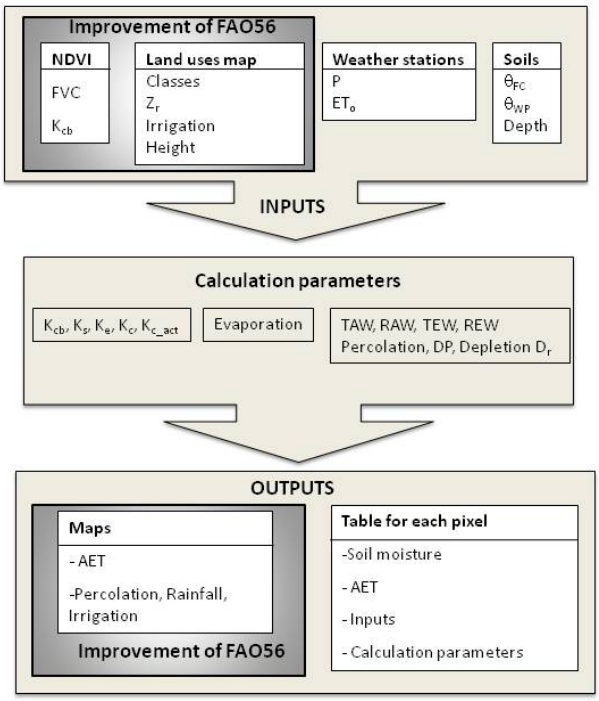

Figure 2. Schema of the FAO56 procedure in the HIDROMORE application. TAW, RAW, TEW, REW expressed water limits of the soil in the root zone (TAW and RAW) and at surface (TEW, REW). All other parameters are defined in the text.

3.2.2 HIDROMORE: HIDROMORE is a computerized tool for estimating evapo-transpiration and aquifer recharge based on FAO56 methodology in a distributed way. This application proposes an improvement of this methodology by incorporating the spatial databases (NDVI, lu/lc map, soil and climatic maps) and using them to parametrize the calculation. Thus, HIDROMORE transforms the water budget of FAO56 into a spatially distributed balance, and the resulting parameters can be studied as raster maps. The temporal scale (daily) and the distributed nature of the simulation (maps) make it adequate for a good management of water resources.

HIDROMORE uses the lu/lc map to compute some parameters of the model, as stated before. The NDVI has been used to calculate the K_{cb} according to the formula of Bausch and Neale (1987). NDVI was also the basis of the FVC calculation, following the observations on barley by González-Piqueras (2006).

$$K_{cb}=1.36\ NDVI-0.03 \quad (3)$$

$$FVC=1.19\ NDVI-0.16 \quad (4)$$

Both methods applied an empirical linear relationship. Even though the NDVI-K_{cb} equation can be different depending on the vegetation cover type, only the relationship for grassland was used for the entire area, owing to the prevalence of this cover (84%). Relationships for other crops such as vineyards are being studied for future research with in situ measurements.

4. RESULTS AND DISCUSSION

The distributed balance afforded a daily maps series of the results: AET, DP and I. Accumulated values can also be extracted (Figure 3). The map spatial sampling matches the Landsat spatial resolution, and for each pixel, the parameter takes a digital floating number corresponding to the parameter value. The influence of the soil database (tiles of 3x3km) is noticeable in the appearance of such maps.

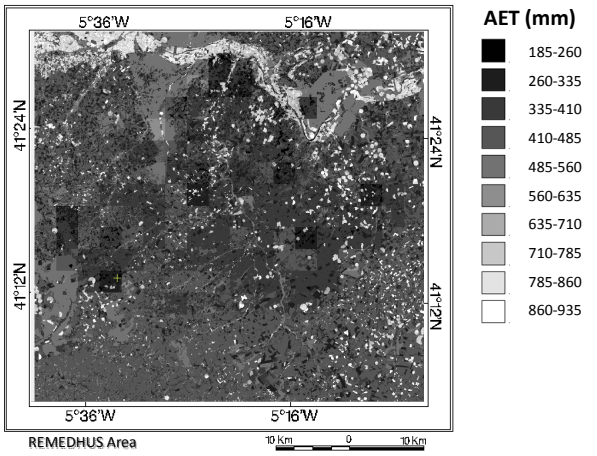

Figure 3. Map of accumulated AET in 2002.

Qualitative analysis was done for each class of the lu/lc map, extracting monthly and annual AET and DP (Table 4). The categories with higher evapotranspiration were irrigated crops and forest-pasture. The highest percolation was for irrigated crops and vineyards, due to their shorter growing period, together with more sandy soil texture in these categories. Irrigation maps can be used to extract the amount of theoretical irrigation water of each plot of this coverage. The mean irrigation amount in 2002 for the whole coverage was 458 mm (maximum is 656 mm and minimum 75 mm).

	AET (mm)	DP (mm)
Forest-pasture	533.30	9.00
Irrigated crops	809.13	183.44
Rainfed cereals	413.42	69.25
Vineyard	327.55	164.95

Table 4. Total AET and DP for lu/lc categories in 2002.

The monthly values showed that the highest evapotranspiration was for irrigated crops in summer –its growing period (Figure 5). For rainfed cereals, the full activity period was spring, when they consumed the natural precipitations and the water reserves of soil. For vineyard and forest-pasture, this period is delayed until the beginning of summer.

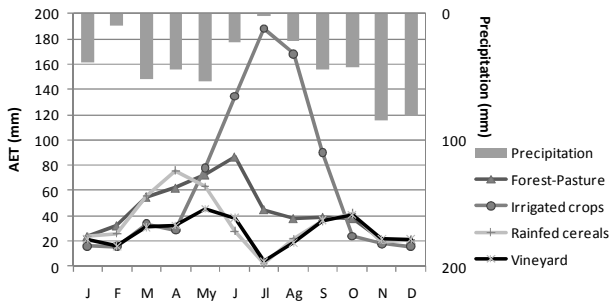

Figure 5. Montly AET for every lu/lc.

The quantitative map assessment was done by means of the simulated soil moisture against the field soil moisture at the REMEDHUS stations. Analysis of RMSE, R, and AI (Willmott, 1987) for 23 stations was performed. HIDROMORE afforded good results for the stations-average soil moisture (R=0.82; AI=0.90; RMSE=0.020 cm^3cm^{-3}), especially for rainfed cereals (R=0.91; AI=0.92; RMSE=0.024 cm^3cm^{-3}).

Regarding the maps, the gridded shape of them (Figure 3) shows the dependency of the water balance on the parameters of soils, particularly θ_{FC} and θ_{WP}. When these values were very low or very high for one cell, they afforded extremes values of evapotranspiration or percolation in this cell, producing a discontinuity.

5. CONCLUSIONS

Some results of a distributed water balance model based both on FAO56 and remotely sensed data were presented in this paper. The integration of the remotely sensed data afforded a detailed description of some vegetation parameters used in the calculation, otherwise these parameters should be tabulated under the FAO56 premises. The model outputs were maps of evapotranspiration, percolation and irrigation rates together with a soil moisture simulation over an area of 1300 km^2. Pre-processing of image consisted, despite more complex alternatives, on orthorectification by physical model, radiometric calibration and correction with standard conditions of atmosphere and DOS method, and topographic correction. Supervised classification had the best accuracy for extracting the lu/lc map. The results showed a good agreement between simulated and field soil moisture in terms of RMSE, AI and R. The maps qualitative analysis agrees with the expected behaviour of the agricultural uses in the area. The parameters that had more influence in the spatial distribution of the balance were θ_{FC} and θ_{WP}, related with the high spatial variability of soils. HIDROMORE improves FAO56 in integrating remotely sensed data and it affords maps of hydrological variables that are very useful for agricultural management. Future research will be done on simulated soil moisture maps *vs.* other image products of this parameter, i.e. SMOS Level 2 products.

REFERENCES

Allen, R.G., Pereira, L.S., Raes, D. and Smith, M., 1998. *Crop Evapotranspiration*. FAO Irrigation and Drainage, 56. Food and Agriculture Organization, Rome.

Bausch, W.C. and Neale, C.U., 1987. Crop coefficients derived from reflected canopy radiation: a concept. Transactions American Soc. Agric, 30(3), pp. 703-709.

Cihlar, J., Ly, H. and Xiao, Q., 1996. Land Cover Classification with AVHRR Multichannel Composites in Northern Environments *Remote Sens. Environ.*, 58, pp. 36-51.

Chavez, P.S., Jr., 1989. Radiometric calibration of Landsat Thematic Mapper multispectral images. *Photogramm. Eng. Rem. S.*, 55(9), pp. 1285-1294.

González-Piqueras, J., 2006. Evapotrans-piración de la Cubierta Vegetal Mediante la Determinación del Coeficiente de Cultivo por Teledetección. Extensión a Escala Regional: Acuífero 08-29 Mancha Oriental., Universitat de Valencia, Valencia, 334 pp.

Hu, C., Muller-Karger, F.E., Andrefouet, S. and Carder, K.L., 2001. Atmospheric correction and cross-calibration of LANDSAT-7/ETM+ imagery over aquatic environments: A multiplatform approach using SeaWiFS/MODIS. *Remote Sens. Environ.*, 78(1-3), pp. 99-107.

Lillesand, T.M. and Kiefer, R.W., 1999. *Remote sensing and image interpretation*. John Wiley and Sons, New York, 384 pp.

Martínez-Fernández, J. and Ceballos, A., 2005. Mean soil moisture estimation using temporal stability analysis. *J. Hydrol.*, 312, pp. 28-38.

Pons, X. and Solé-Sugrañés, L., 1994. A Simple Radiometric Correction Model to Improve Automatic Mapping of Vegetation from Multispectral Satellite Data. *Remote Sens. Environ.*, 48, pp. 191-204.

Toutin, T., 2004. Geometric Processing of Remote Sensing Images: Models, Algorithms and Methods (review paper). *Int. J. Remote Sens.*, 25 (10), pp. 1893-1924

Vincent, S. and Pierre, F., 2003. Identifying Main Crop Classes in an irrigated area using High Resolution Image Time Series, IGARSS 2003, pp. 252 - 254.

Wegehenkel, M. and Kersebaum, K.C., 2005. The validation of a modelling system for calculating water balance and catchment discharge using simple techniques based on field data and remote sensing data. *Phys. Chem. Earth*, 30, pp. 171-179.

Willmott, C.J., 1982. Some comments on the evaluation of model performance. *B. Am. Meteorol. Soc.*, 63, pp. 1309−1313.

Wolfe, R.E. Masahiro, N., Fleig, A. J., Kuyper, J. A., Roy, D. P. and Storey, J. C., 2002. Achieving sub-pixel geolocation accuracy in support of MODIS land science. *Remote Sens.* Environ., 83, pp. 31– 49.

ACKNOWLEDGEMENTS

MORE and EBHE Project are funded by the projects REN2003-02956/HID and CGL2008-04047 (Spanish Plan of Science and Technology). This work would not have been possible without aid from projects ESP2006-00643 and ESP2007-65667-C04-04 from the Spanish Ministry of Science and Technology, and AGRHIMOD from the Junta de Castilla y León. The authors also wish to thank the STIG of the University of Salamanca for providing satellite images and other cartographic data and the Regional Government of Castilla y León for the SIGPAC information.